Surface Science 647 (2016) 45–50

Contents lists available at ScienceDirect

Surface Science

journal homepage: www.elsevier.com/locate/susc

First-principles study on reconstruction of 4H-SiC(0001) and (000$\bar{1}$)

Tomoaki Kaneko [a,b,*], Takahiro Yamasaki [a,b], Nobuo Tajima [a,b,c], Takahisa Ohno [a,b,c]

[a] Computational Material Science Unit, National Institute for Materials Science (NIMS), Tsukuba, Ibaraki 305-0047, Japan
[b] Materials Research Consortium for Energy Efficient Electronic Devices (MARCEED), Tsukuba, Ibaraki 305-0047, Japan
[c] Institute for Industrial Science, University of Tokyo, Meguro, Tokyo 153-8505, Japan

ARTICLE INFO

Article history:
Received 1 October 2015
Accepted 22 November 2015
Available online 2 December 2015

Keywords:
4H-SiC
π-bonded chain model
First-principles calculations

ABSTRACT

We have found that 4H-SiC(0001) and (000$\bar{1}$) surfaces can reconstruct to stable (2×1) π-bonded chain structures, which are the same kind of structure that was predicted by Pandey for Si(111) surface (K. C. Pandey, 1981) but have not been examined for the SiC surfaces so far. Their relative energy gain on (0001) and (000$\bar{1}$) surfaces to the ideal spin non-polarized surfaces are 0.275–0.298 eV/(1×1) and 0.378–0.441 eV/(1×1), respectively. The band gaps of the π-bonded chain models for 4H-SiC(0001) and (000$\bar{1}$) are 1.34–1.36 eV and 1.92–2.46 eV, respectively, which are much larger than that for Si(111) due to difference between energy levels of *p*-orbitals of Si and C atoms.

1. Introduction

Silicon carbide (SiC) is one of the promising materials for high-power and high-temperature device applications owing to its fascinating physical properties such as wide bandgaps and high thermal stabilities. There are several SiC polytypes which are specified by the stacking order of SiC bilayer, and the cleaved SiC surfaces, in which either Si or C atoms can be up at the surface SiC bilayer, that is, the (111) surface of 3C- and (0001) surfaces of 4H- and 6H-SiC are widely used for devices application. The surface structures are changed by annealing temperatures and by Si flux supplied after surface exposure by cleavage, and also the surface Si/C ratios often deviate from stoichiometry.[1] Several surface super structures such as (1×1), $(\sqrt{3} \times \sqrt{3})$, (3×3), and $(6\sqrt{3} \times 6\sqrt{3})$ for Si-face, and (1×1), (2×2), and (3×3) for C-face were reported [1]. Although the identification of atomic surface structures is crucial to understand the surface electronic properties and reactions which are involved in device fabrication, both experimental and theoretical studies for the cleaved SiC surfaces are still insufficient for complete understanding as mentioned below.

A few theoretical studies were carried out using first-principles calculations for the stoichiometric SiC surfaces such as 3C-SiC(111), 4H-SiC(0001), and 6H-SiC(0001). For the C-faces, e.g., 3C-SiC($\overline{111}$) and 6H-SiC(000$\bar{1}$), the downward displacements of the topmost C atoms were reported [2, 3, 4, 5, 6]. For the Si-face, on the other hand, one paper reports that the topmost Si atoms show a buckled reconstruction with (2×1) periodicity in 4H-SiC(0001)[7].

Experimentally, Starke et al. performed low-energy electron diffraction (LEED) and core level photo electron spectroscopy for the cleaved 6H-SiC(0001) and (000$\bar{1}$) surfaces and observed (2×1) reconstruction [8]. Such the (2×1) reconstruction was observed also in 4H-SiC(0001) surface using reflection high-energy electron diffraction (RHEED) [9]. The (2×1) buckled structure on the Si-face proposed by the theoretical calculation[7] is not conclusive to explain the experiments, since such the proposed model is difficult to be distinguished from an ideal (1×1) surface through LEED or RHEED patterns [9]. Starke et al. interpreted the (2×1) reconstruction not as the buckled structure but as the so-called π-bonded chain (π-BC) structure which was predicted by Pandey for Si(111)[10]. However, the stability of the (2×1) π-BC has not been examined theoretically for the SiC surfaces. In this paper, we consider 4H-SiC with the largest bandgaps among 3C, 4H, and 6H polytypes and investigate the (2×1) reconstruction of the 4H-SiC(0001) and (000$\bar{1}$) surfaces by using first-principles calculations.

2. Computational details

We performed first-principles calculations based on the density functional theory [11, 12] within generalized gradient approximation [13] (GGA) using PHASE/0 code [14]. We performed both spin unpolarized and polarized calculations. Ultrasoft pseudo potential [15] is used for C atoms and norm-conserving ones [16] are used for H and Si atoms. The cutoff energies of planewave expansions for wave functions and charge density are chosen as 25 and 255 Ry, respectively. The optimized lattice constants of 4H-SiC are $a = 3.097$ Å and $c = 10.125$ Å, which are 0.77% and 0.73% larger than those of experimental values [17], respectively. As shown in Fig. 1(a), there are two inequivalent planes in 4H-SiC perpendicular to the surfaces. We shall use the *h*–*k*

* Corresponding author.
E-mail address: KANEKO.Tomoaki@nims.go.jp (T. Kaneko).

http://dx.doi.org/10.1016/j.susc.2015.11.019
0039-6028/

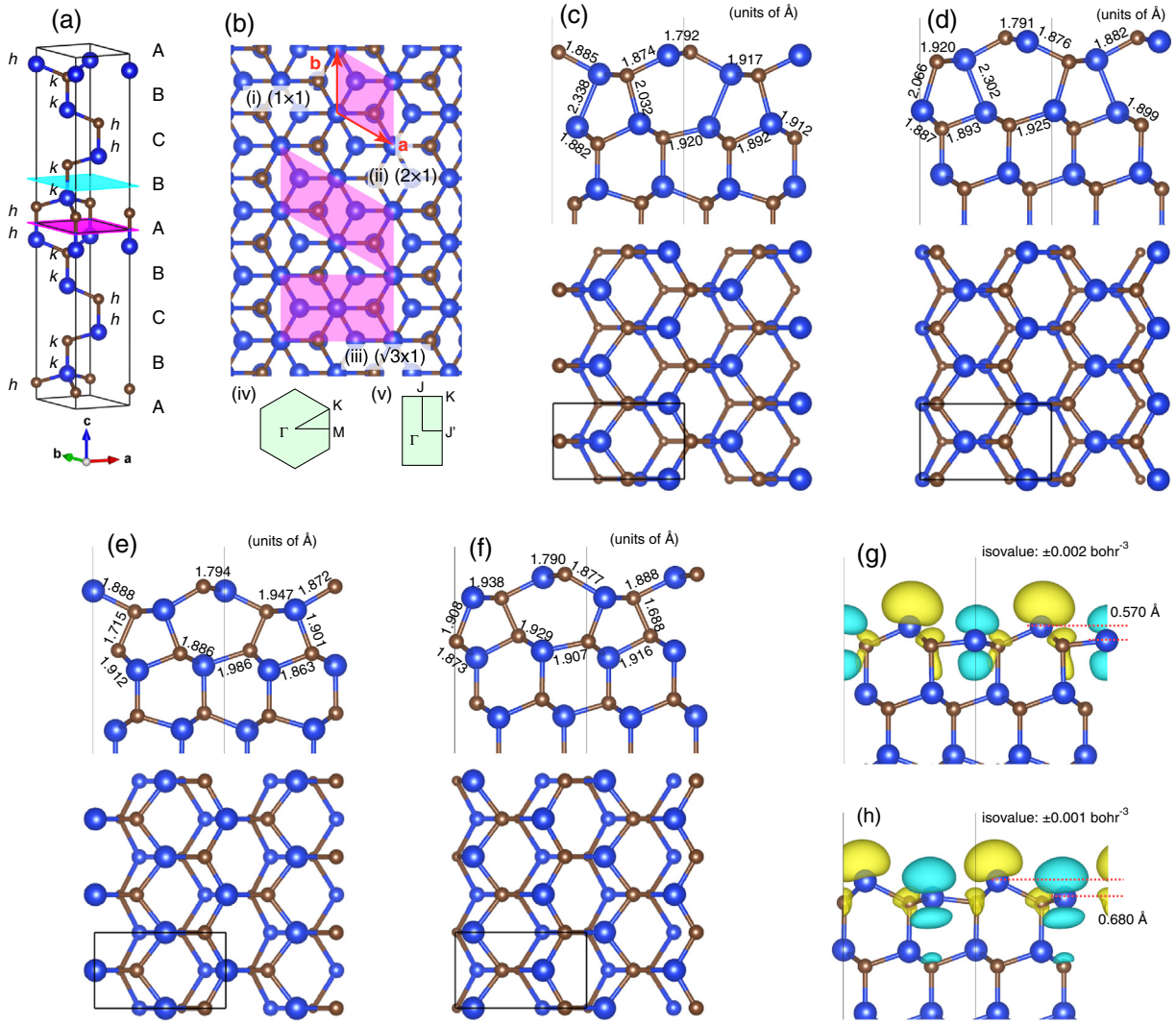

Fig. 1. (a) Lattice structure of 4H-SiC. The blue and brown balls represent Si and C atoms, respectively. In 4H-SiC, there are two inequivalent terminations indicated by the light red plane (*h*-termination) and light blue plane (*k*-termination). (b) Surface unit cell used in this study for (i) (1×1), (ii) (2×1), and (iii) $(\sqrt{3}\times1)$, and corresponding Brillouin zone for (iv) (1×1), and (v) $(\sqrt{3}\times1)$. (c) Side and top views of π-BC model in 4H-SiC(0001) at the *h*-termination. (d) Same figure as (c) for the *k*-termination. (e) Side and top views of π-BC model in 4H-SiC$(000\bar{1})$ at the *h*-termination. (f) Same figure as (e) for the *k*-termination. (g) The buckled model obtained within spin polarization for 4H-SiC(0001) at the *h*-termination. The contour plot is corresponding spin density. (h) Same figure as (g) for the *k* -termination. The side views of surface models shown in this figure are view from $[01\bar{1}0]$ direction. (For interpretation of the references to color in this figure legend, the reader is referred to the web version of this article.)

notation introduced by Jagodzinski[18] to specify the surface termination. Note that the cleaved surface at *h*-site (*h*-termination) has the stacking order of A-B-C-B- ⋯ (*k*-site like stacking) below the surface, and the other cleaved surface at *k*-site (*k*-termination) has the stacking order of B-A-B-C- ⋯ (*h*-site like stacking).

We use repeated slab models, each of which contains a SiC slab and a vacuum region thicker than 10 Å in the unit cell. To discuss the termination dependence of stability, the slabs consist of eight and nine SiC bilayers for the *k*- and *h*-terminated models, respectively. Each of the back surface atoms is passivated by single H atom. The position of atoms in the upper five SiC bilayers was optimized until residual forces became less than 5×10^{-4} Hartree/bohr. We have two kinds of surface unit cells depending on the reconstruction model periodicities as shown in Fig. 1(b). We took $8\times8\times1$ and $4\times8\times1$ special *k*-point sets [19] in the Brillouin zone for the 1×1 and $\sqrt{3}\times1$ surface unit cells, respectively. Besides the GGA method, we have also employed the Heyd–Scuseria–Ernzerhof (HSE06) hybrid functional [20,21] for exchange and correlation to estimate more reliably the band gaps of some important surfaces models based on the GGA optimized structures using $6\times12\times1$ Γ-point centered uniform mesh.

3. Results and discussion

3.1. Models and stability

Table 1 lists all the calculated structures and the calculated total energy differences (ΔE), taking the energy of the ideal structure for each surface as a reference. Spin polarized and unpolarized geometry calculations were performed to obtain three types of structures, i.e., the ideal structure, the π-BC structure, and the buckled structure, on both Si- and C-faces of 4H-SiC. In the ideal structures, the topmost Si/C atoms are three coordinated and thus have a dangling bond. In the π-BC structures, as shown in Figs. 1(c–f), the six member rings between the topmost two bilayers in the ideal structures are reorganized to five and seven member rings and the three coordinated atoms, i.e. the topmost Si and C atoms in the seven member ring, are spatially close enough to